0^9

N91-30223

# KEY RESULTS OF THE MINI-DOME FRESNEL LENS CONCENTRATOR ARRAY DEVELOPMENT PROGRAM UNDER RECENTLY COMPLETED NASA & SDIO SBIR PROJECTS

Mark J. O'Neill
ENTECH, Inc.
DFW Airport, TX

Michael F. Piszczor
NASA Lewis Research Center
Cleveland, OH

Lewis M. Fraas
Boeing High Technology Center
Seattle, WA

## INTRODUCTION

Since 1986, ENTECH and the NASA Lewis Research Center have been developing a new photovoltaic concentrator system for space power applications. The unique refractive system uses small, dome-shaped Fresnel lenses to focus sunlight onto high-efficiency photovoltaic concentrator cells which use prismatic cell covers to further increase their performance. Under Small Business Innovation Research (SBIR) funding provided by both NASA and SDIO, the mini-dome Fresnel lens concentrator array has progressed from a paper concept in 1986 to functional array hardware in 1990-91. Since 1989, Boeing has been a key participant in the development of this concept, providing both record-breaking GaAs/GaSb tandem cell technology and significant expertise in the development of the panel structure and related manufacturing techniques. Other project participants include 3M Company (lens tooling); Fresnel Optics (prism cover tooling); and Varian Associates (GaAs cells).

Highlights of the five-year development include near-AM0 Lear Jet flight testing of mini-dome lenses (90% net optical efficiency achieved); tests verifying sun-pointing error tolerance with negligible power loss; simulator testing of prism-covered GaAs concentrator cells (24% AM0 efficiency); testing of prism-covered Boeing GaAs/GaSb tandem cells (31% AM0 efficiency); and fabrication and outdoor testing of a 36-lens/cell element panel. These test results have confirmed previous analytical predictions which indicate substantial performance improvements for this technology over current array systems. Based on program results to date, it appears that an array power density of 300 watts/square meter and a specific power of 100 watts/kilogram can be achieved in the near term. All components of the array appear to be readily manufacturable from space-durable materials at reasonable cost. This paper presents a concise review of the key results leading to the current array, and briefly discusses further development plans for the future.

## SYSTEM DESCRIPTION

Figures 1 through 4 show the basic mini-dome Fresnel lens space concentrator array concept. Small, square-aperture, thin, dome-shaped Fresnel lenses focus incident sunlight by a factor of about 100 onto circular photovoltaic cells. The cells are mounted to a backplane radiator for waste heat rejection. Individual lenses are placed within slots in a honeycomb panel, which is structurally integrated with the backplane radiator. Cells are interconnected in series/parallel circuits to build up the desired voltage, current, and power values for the panel. Panels are mounted onto automatically deploying support structures to form large, multi-kilowatt arrays.

Material selection has been one of the key issues in the development of the mini-dome lens array. The current materials have been chosen based on previous successful space use, ease-of-fabrication, and cost. The lens is a laminated assembly of ceria-doped microglass over clear silicone rubber, as shown in Figure 5. The honeycomb and radiator are both made from aluminum. The cell is a tandem structure of gallium arsenide over gallium antimonide, to maximize array performance. The cells use silicone rubber prismatic covers to eliminate grid shading losses, thereby enhancing performance. As discussed in the following section, prototype lenses, cells, prismatic covers, and panels have all been successfully fabricated and tested.

## KEY RESULTS

The unique dome lens design is shown in Figure 6. While every prism in the lens is different from all others, each prism is configured for symmetrical refraction. Specifically, the angle of incidence of the solar rays on the outer smooth surface of the lens is equal to the angle of emergence of these solar rays on the faceted inner surface of the lens. This symmetry minimizes reflection losses, thereby maximizing efficiency. Furthermore, this symmetry greatly improves image quality compared to conventional flat Fresnel lenses. Even more importantly, this refraction symmetry vastly expands allowable inaccuracies encountered in both initial manufacture and long-term operation. Remarkably, the slope error tolerance of the mini-dome lens is more than 100 times larger than for a flat Fresnel lens, and more than 200 times larger than for a reflective concentrator, for equal image defocussing.

By "tweaking" the angles of the individual prisms making up the Fresnel pattern, the dome lens has been designed to focus the sunlight into a circular spot about 2.6 mm in diameter, which is smaller than the cell diameter of 4.0 mm by an amount which was selected to allow a sun-pointing error of 1 degree without loss of power output. Performance goals for the lens were >90% net optical efficiency and $\pm 1$ degree tracking error tolerance with negligible loss of power. Measurements on a pure silicone lens (no glass superstrate) with a square aperture mask coupled with a gallium arsenide cell are shown in Figure 7. Note that the lens indeed achieved 90% efficiency. Note also that the power loss at 1 degree tracking error is only 1%. Later lenses with prototype glass superstrates have achieved about 85% optical efficiency with less than 5% power loss at 1 degree tracking error. Further improvement in the glass superstrates is expected to raise the laminated lens performance back to the pure silicone lens levels. Still higher performance should be achievable through the use of antireflection coatings on the glass superstrate.

Figure 8 shows the Boeing-developed tandem cell approach. The prism-covered gallium arsenide top cell converts about 24% of the available sunlight to electricity. The top cell energy conversion occurs for that portion of the solar spectrum below about 0.9 micron in wavelength. Longer, infrared wavelengths pass through the top cell onto the prism-covered gallium antimonide bottom cell. The bottom cell converts another 7% of the available sunlight to electricity, for a total tandem cell efficiency of 31%. This value has been confirmed by NASA-Lewis via Lear Jet flight tests coupled with flash solar simulator tests. Higher efficiency values are anticipated in the future, as the newly developed gallium antimonide cell technology matures.

Thermal analyses have been conducted to predict on-orbit cell operating temperature. Figure 9 shows a typical thermal analysis result for the hottest portion of a low earth orbit (LEO) mission. The radiator temperature just beneath the cell is about 96C. Thus, with a well designed cell-to-radiator mount (with a 4C gradient), the cell temperature should be about 100C. Figure 10 shows a similar result for a geosynchronous earth orbit (GEO) mission. The cell temperature will be about 76C for GEO operation.

Mass analyses have been conducted to estimate mass per unit area for the baseline panel, as shown in Figure 11. A value of about 2.4 kg/sq.m. appears achievable in the very near term. Furthermore, automatically deploying support structures designed by others have been identified for use with the mini-dome lens panels. These structures have a mass of about 0.7 kg/sq.m., for a total array mass density of 3.1 kg/sq.m. This array mass density is approximately equivalent to the planned one-sun Kapton blanket array for the Space Station Freedom. Thus, the mini-dome lens array is extremely light-weight.

Figure 12 summarizes the near-term significance of the previously discussed performance and mass parameters. With single junction cells, power density values of 250-260 W/sq.m. will be achieved. With tandem cells, power density values of 300-330 W/sq.m. will be achieved. With single-junction cells, specific power values above 80 W/kg will be achieved. With tandem cells, specific power values above 100 W/kg will be achieved.

## PROTOTYPE PANELS

Over the past year, several prototype panels have been successfully made and tested. The most recent panel is shown in Figure 13. Boeing has developed a computer-controlled milling process for rapidly producing extremely rigid, light-weight, thermally efficient radiator/honeycomb assemblies from a plate of aluminum. Cell assemblies are mounted directly to the panel backplane, while individual lenses are attached to the front of the panel structure. Outdoor testing of these panels has shown performance levels close to expectations for the lenses and cells utilized. These prototype panels have convinced the project participants of the practicality of the mini-dome lens panel concept.

## CONCLUSION

The mini-dome lens array development has progressed successfully to the prototype hardware stage. Performance measurements have closely matched expectations. A small array space flight test is planned for 1992 in conjunction with the PASP+ program (as discussed by Guidice et al in another paper at this conference). Independent comparative array analyses are confirming the relative merits of the new array technology (e.g., as discussed by Kraus in another paper at this conference). Figure 14 summarizes the key features and advantages of the mini-dome Fresnel lens space concentrator approach.

Fig. 1

**DOME LENS PV MODULE CONCEPTUAL DESIGN**

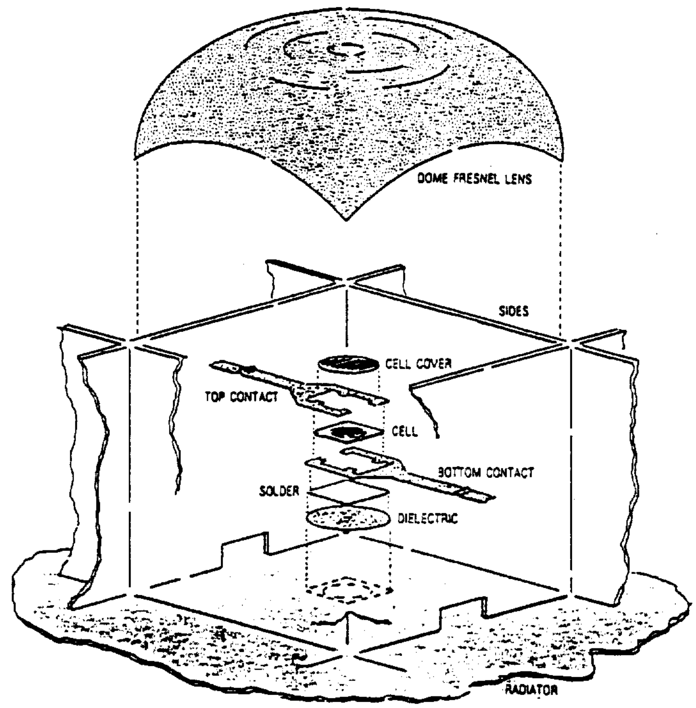


Fig. 2

ENTECH DOME LENS PV CONCENTRATOR PANEL CONCEPTUAL DESIGN

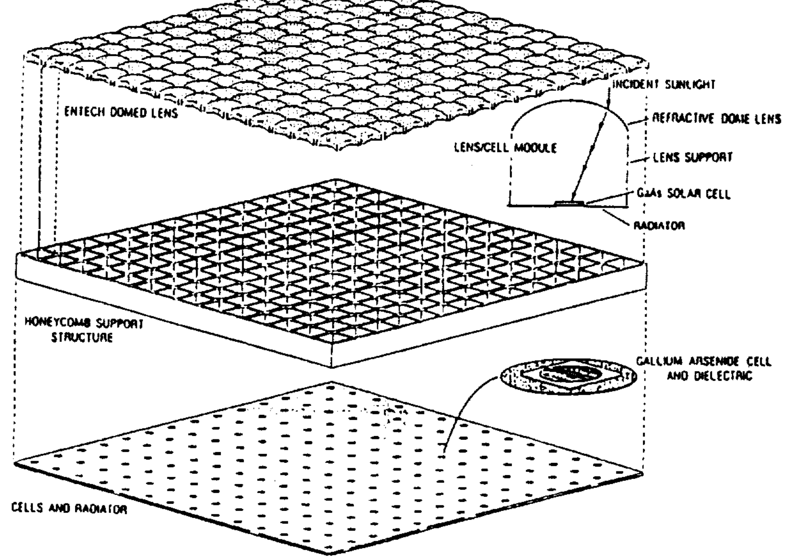

Fig. 3 CROSS - SECTIONAL VIEWS OF DOME LENS PV PANEL

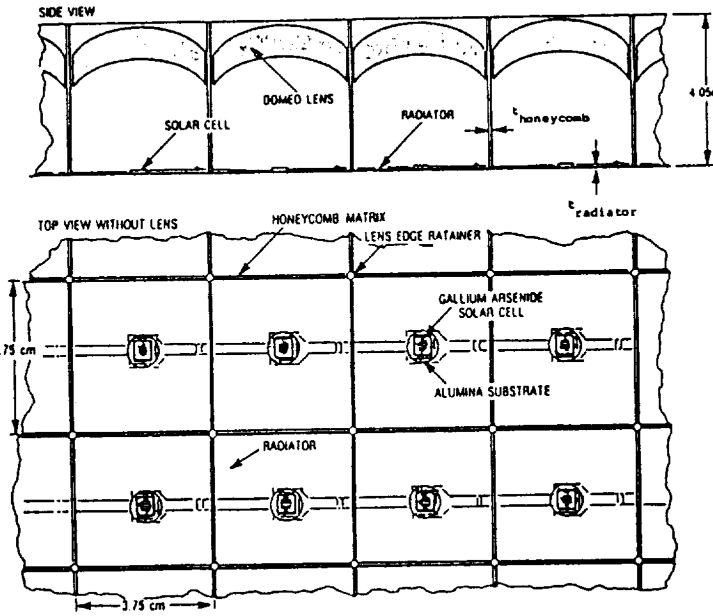


Fig. 4 DOME LENS PV ARRAYS ON ESS SYSTEM ATTACHED TO SPACE STATION

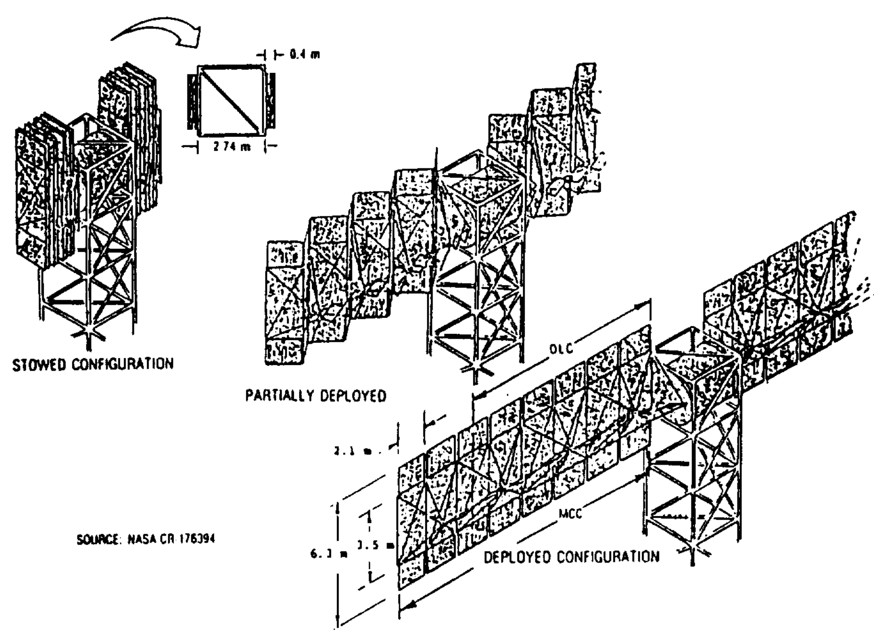

Fig. 5

BASELINE LENS DESIGN FOR LOW-EARTH-ORBIT (LEO) APPLICATIONS
(MICROGLASS SHIELDS POLYMERIC LENS FROM ATOMIC OXYGEN)

LAMINATED CERIA MICROGLASS/SILICONE RTV
MINI-DOME FRESNEL LENS

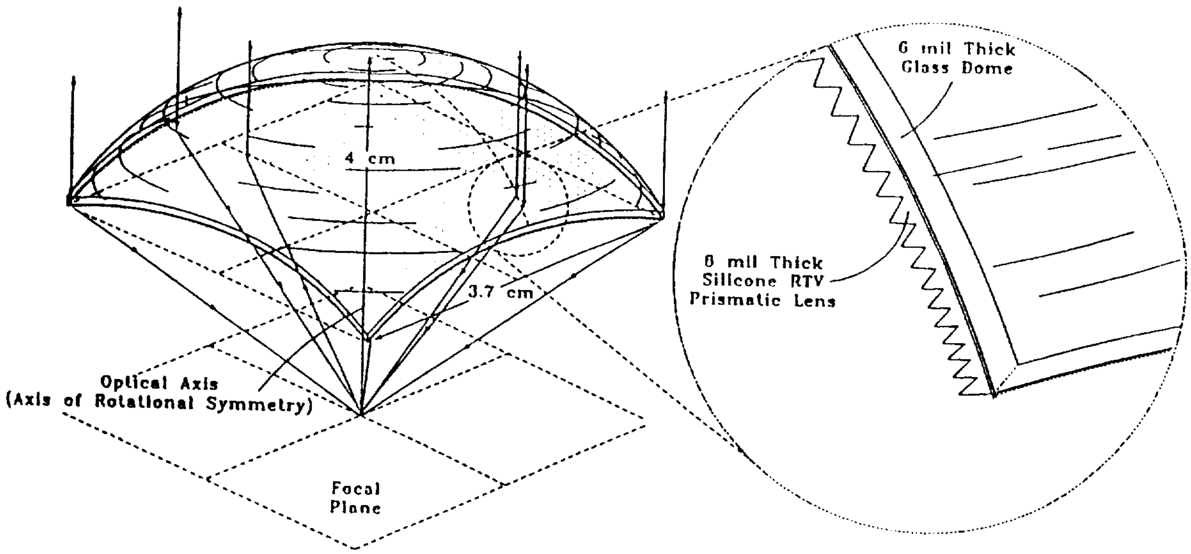


Fig. 6

MAGNIFIED VIEW OF SEVERAL PRISMS WITHIN THE ENTECH DOME LENS, SHOWING REFRACTION SYMMETRY AND BLUNT TIP TOLERANCE

THIS SYMMETRICAL REFRACTION CONDITION MINIMIZES REFLECTION LOSSES FOR A GIVEN RAY TURNING ANGLE, THEREBY MAXIMIZING TRANSMITTANCE.

THE SYMMETRICAL REFRACTION CONDITION ALSO MINIMIZES IMAGE SIZE AND MAXIMIZES TOLERANCE FOR MANUFACTURING ERRORS AND ABERRATIONS.

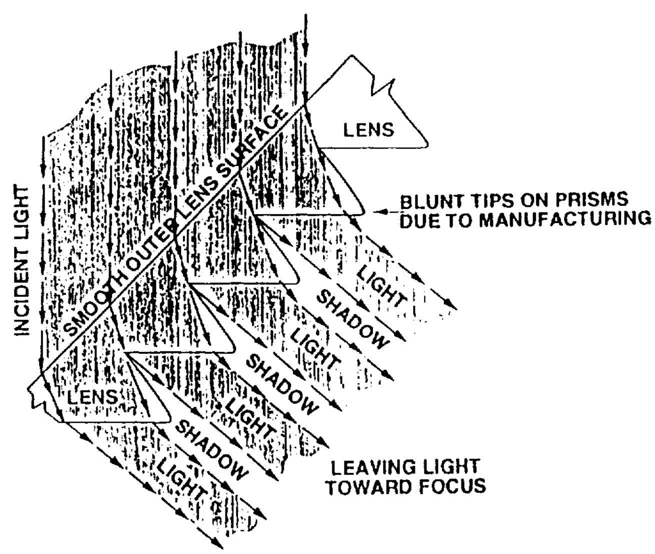

## NASA LEWIS LEAR JET HIGH ALTITUDE TEST FACILITY MEASURED LENS PERFORMANCE FOR MODULE #1

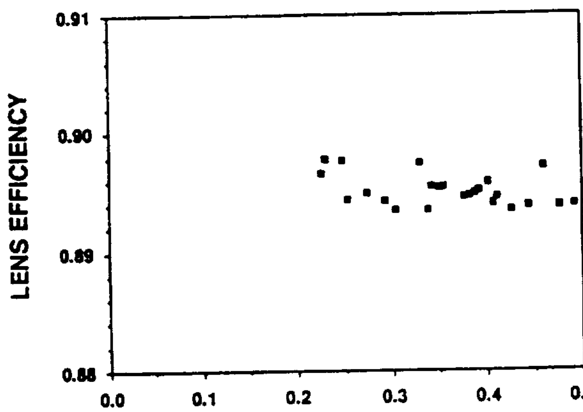


(Prototype Silicone Rubber Lens,
Masked to Simulate Square Aperture
Flown March 1990)

## TRACKING ERROR PERFORMANCE TEST FOR PROTOTYPE MODULE #1

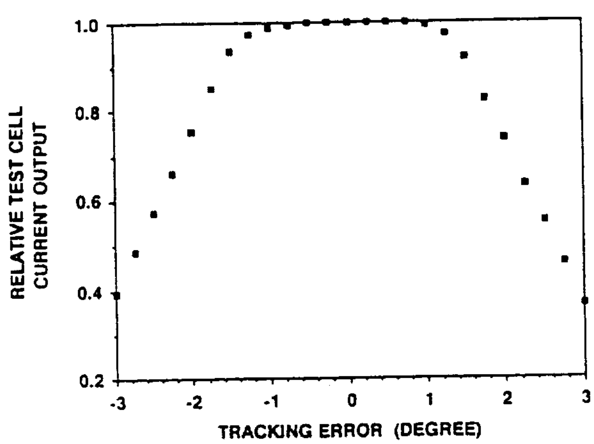


LENS/CELL ELEMENT DESIGNED
FOR 1 DEGREE TRACKING ERROR TOLERANCE

(Prototype Silicone Rubber Lens,
Masked to Simulate Square Aperture)

Fig. 7

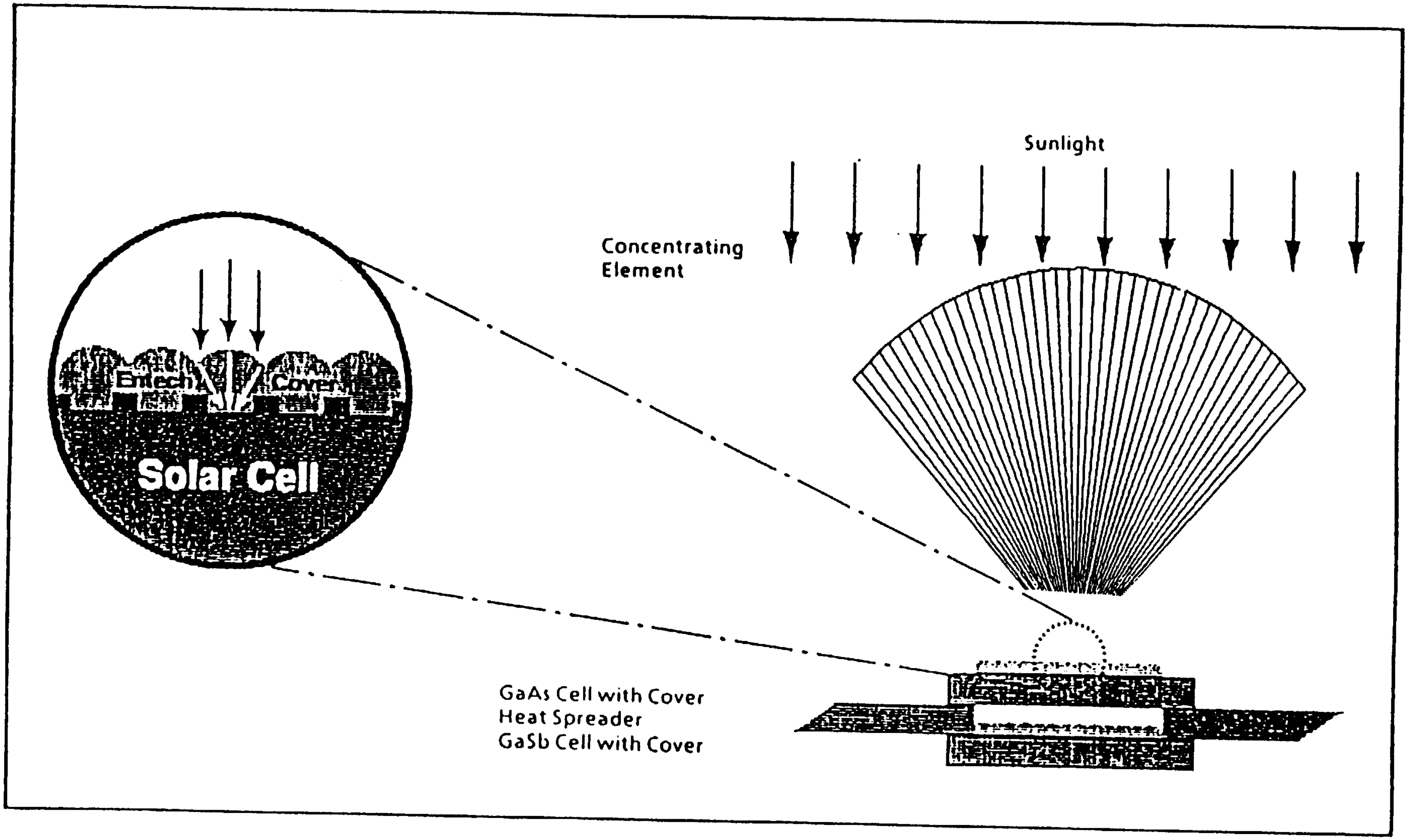


*GaAs/GaSb Concentrator Cell Concept*

Fig. 8

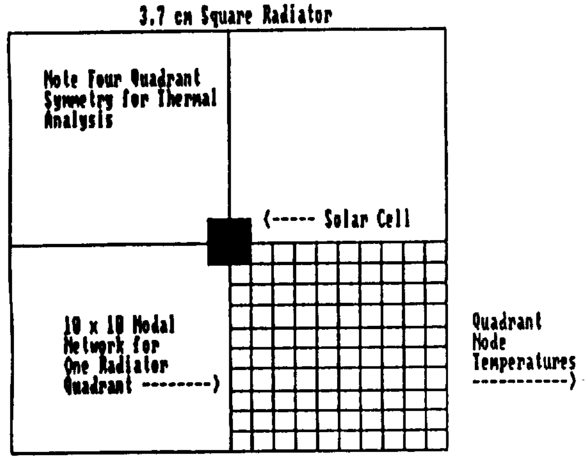


**ASSUMPTIONS**

Thermal Control Coating on Both Sides of Radiator:
    Solar Absorptance = 0.20, Infrared Emittance = 0.90

Aluminum Radiator:
    Thermal Conductivity = 173 W/m-K

Glass/Silicone Lens on Front Side of Radiator:
    Solar Transmittance = 0.92, Infrared Emittance = 0.90

Hottest Portion of Low Earth Orbit (LEO):
    Radiator Facing Earth, Lens Facing Sun
    Earth Albedo Reflectance = 0.36
    Earth Effective Radiation Temperature = 255K
    Radiator-to-Earth View Factor = 0.922

Solar Constant = 1371 W/sq.m.

Prism-Covered GaAs Cell:
    Solar Absorptance = 0.95
    Electrical Conversion Efficiency = 0.20
    Cell Area = 0.01 Times Lens Area

Net Waste Heat Rate from Cell To Radiator = 1.30 W
    (3.7 cm x 3.7 cm x 0.1371 W/sq.cm. x 0.92 x (0.95 - 0.20))

| | | | | | | | | | |
|---|---|---|---|---|---|---|---|---|---|
| 95.910 | 91.381 | 88.713 | 86.947 | 85.697 | 84.787 | 84.125 | 83.660 | 83.364 | 83.219 |
| 91.381 | 89.621 | 87.910 | 86.526 | 85.452 | 84.631 | 84.019 | 83.583 | 83.302 | 83.165 |
| 88.713 | 87.910 | 86.876 | 85.890 | 85.045 | 84.360 | 83.828 | 83.441 | 83.188 | 83.063 |
| 86.947 | 86.526 | 85.890 | 85.208 | 84.572 | 84.025 | 83.585 | 83.255 | 83.036 | 82.927 |
| 85.697 | 85.452 | 85.045 | 84.572 | 84.101 | 83.676 | 83.321 | 83.049 | 82.865 | 82.772 |
| 84.787 | 84.631 | 84.360 | 84.025 | 83.676 | 83.349 | 83.066 | 82.844 | 82.692 | 82.615 |
| 84.125 | 84.019 | 83.828 | 83.585 | 83.321 | 83.066 | 82.840 | 82.659 | 82.533 | 82.469 |
| 83.660 | 83.583 | 83.441 | 83.255 | 83.049 | 82.844 | 82.659 | 82.509 | 82.403 | 82.349 |
| 83.364 | 83.302 | 83.188 | 83.036 | 82.865 | 82.692 | 82.533 | 82.403 | 82.311 | 82.263 |
| 83.219 | 83.165 | 83.063 | 82.927 | 82.772 | 82.615 | 82.469 | 82.349 | 82.263 | 82.218 |

Fig. 9 Thermal Analysis Results for Low Earth Orbit (LEO) for 200 Micron (8 mil) Radiator Thickness

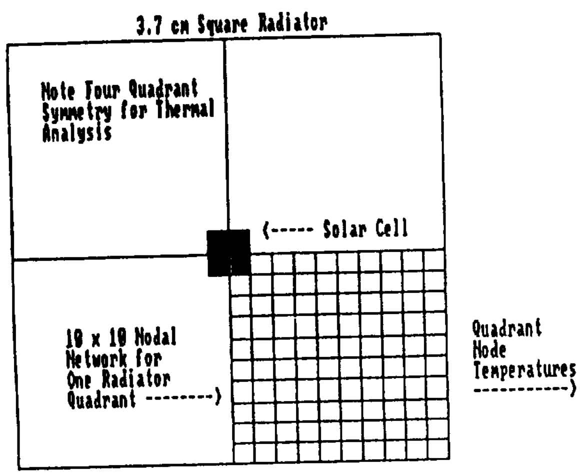


**ASSUMPTIONS**

Thermal Control Coating on Both Sides of Radiator:
    Solar Absorptance = 0.20, Infrared Emittance = 0.90

Aluminum Radiator:
    Thermal Conductivity = 173 W/m-K

Glass/Silicone Lens on Front Side of Radiator:
    Solar Transmittance = 0.92, Infrared Emittance = 0.90

Hottest Portion of Geosynchronous Earth Orbit (GEO):
    Radiator Facing Earth, Lens Facing Sun
    Earth Albedo Reflectance = 0.36
    Earth Effective Radiation Temperature = 255K
    Radiator-to-Earth View Factor = 0.023

Solar Constant = 1371 W/sq.m.

Prism-Covered GaAs Cell:
    Solar Absorptance = 0.95
    Electrical Conversion Efficiency = 0.20
    Cell Area = 0.01 Times Lens Area

Net Waste Heat Rate from Cell To Radiator = 1.30 W
    (3.7 cm x 3.7 cm x 0.1371 W/sq.cm. x 0.92 x (0.95 - 0.20))

| | | | | | | | | | |
|---|---|---|---|---|---|---|---|---|---|
| 72.207 | 67.677 | 65.008 | 63.240 | 61.988 | 61.076 | 60.412 | 59.946 | 59.649 | 59.504 |
| 67.677 | 65.916 | 64.204 | 62.819 | 61.742 | 60.920 | 60.306 | 59.869 | 59.588 | 59.450 |
| 65.008 | 64.204 | 63.170 | 62.182 | 61.335 | 60.648 | 60.116 | 59.727 | 59.474 | 59.349 |
| 63.240 | 62.819 | 62.182 | 61.499 | 60.861 | 60.313 | 59.872 | 59.541 | 59.322 | 59.212 |
| 61.988 | 61.742 | 61.335 | 60.861 | 60.390 | 59.964 | 59.608 | 59.334 | 59.150 | 59.057 |
| 61.076 | 60.920 | 60.648 | 60.313 | 59.964 | 59.635 | 59.351 | 59.129 | 58.976 | 58.899 |
| 60.412 | 60.306 | 60.116 | 59.872 | 59.608 | 59.351 | 59.125 | 58.943 | 58.817 | 58.753 |
| 59.946 | 59.869 | 59.727 | 59.541 | 59.334 | 59.129 | 58.943 | 58.792 | 58.686 | 58.632 |
| 59.649 | 59.588 | 59.474 | 59.322 | 59.150 | 58.976 | 58.817 | 58.686 | 58.593 | 58.545 |
| 59.504 | 59.450 | 59.349 | 59.212 | 59.057 | 58.899 | 58.753 | 58.632 | 58.545 | 58.501 |

Fig. 10 Thermal Analysis Results for Geosynchronous Earth Orbit (GEO) for 200 Micron (8 mil) Radiator Thickness

Fig. 11

MINI-DOME LENS SPACE PHOTOVOLTAIC CONCENTRATOR
NEAR-TERM BASELINE PANEL MASS BREAKDOWN

| Element | Material | Density (g/cu.cm.) | Thickness (cm) | Surface Area / Panel Area | Mass/Panel Area (kg/sq.m.) |
|---|---|---|---|---|---|
| Lens Superstrate | Microglass | 2.50 | 0.015 | 1.30 | 0.49 |
| Lens Prisms | Silicone | 1.00 | 0.015* | 1.30 | 0.19 |
| Radiator | Aluminum | 2.77 | 0.020 | 1.00 | 0.55 |
| Cell/Cover/Mount | GaAs et al | 5.70 | 0.046 | 0.02 | 0.05 |
| Honeycomb | Aluminum | 2.77 | 0.015 | 2.20 | 0.91 |
| Radiator Coating | Alumina | 3.88 | 0.001 | 2.00 | 0.08 |
| Miscellaneous | ---------------- 7.5% of Above Total | | | ----------------- | 0.17 |
| TOTAL | | | | | 2.44 |

* Silicone Base Thickness = 0.010 cm
Silicone Prism Thickness = 0.010 cm (But Half Void)
Effective Silicone Thickness = 0.015 cm

Fig. 12

MINI-DOME FRESNEL LENS ARRAY - NEAR-TERM PERFORMANCE ESTIMATES
BASED ON RECENT TEST RESULTS FOR PROTOTYPE CELLS AND LENSES

| ITEM | NEAR-TERM GaAs | NEAR-TERM TANDEM |
|---|---|---|
| Lens Type | Glass/Silicone | Glass/Silicone |
| Panel Type | 0.02 cm Alum. | 0.02 cm Alum. |
| Cell Type | GaAs | GaAs + GaSb |
| Cell Eff. at 25C | 24% | 24% + 7% = 31% |
| Max. LEO Cell Oper. Temp. | 100C | 100C & 100C |
| Cell Eff. at Max. LEO Temp. | 22% | 22% + 5% = 27% |
| Max. GEO Cell Oper. Temp. | 76C | 76C & 76C |
| Cell Eff. at Max. GEO Temp. | 23% | 23% + 6% = 29% |
| Lens Efficiency | 90% | 90% |
| Packing Factor | 97% | 97% |
| Mismatch/Wiring Factor | 93% | 93% |
| LEO Array Efficiency | 18% | 22% |
| LEO Power Density (w/sq.m.) | 247 | 302 |
| GEO Array Efficiency | 19% | 24% |
| GEO Power Density (w/sq.m.) | 260 | 329 |
| Panel Mass (kg/sq.m.) | 2.4 | 2.4 |
| Structure Mass (kg/sq.m.) | 0.7 | 0.7 |
| Array Mass (kg/sq.m.) | 3.1 | 3.1 |
| LEO Specific Power (w/kg) | 80 | 97 |
| GEO Specific Power (w/kg) | 84 | 106 |

Note: Measured Performance Parameters for Prototype Cells and Lenses Are Underlined.

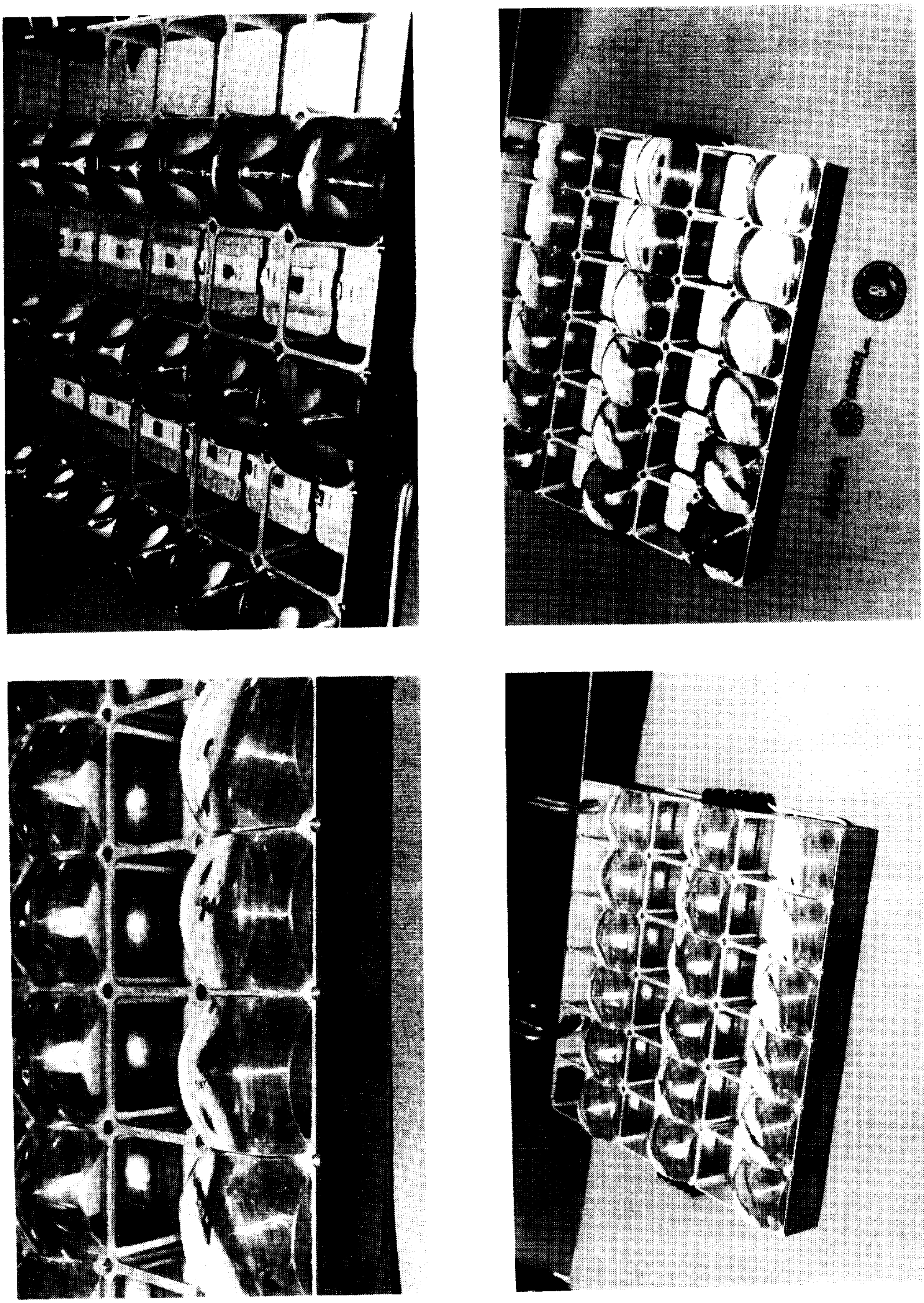

Fig. 13

Fig. 14

MINI-DOME LENS SPACE PHOTOVOLTAIC CONCENTRATOR
KEY FEATURES AND ADVANTAGES

**UNIQUE LENS:** THE TRANSMITTANCE-OPTIMIZED DOME LENS PROVIDES 90% NET OPTICAL EFFICIENCY (WITHOUT THE NEED FOR SECONDARY OR TERTIARY CONCENTRATORS). EXCEPTIONAL TOLERANCES FOR MANUFACTURING AND OPERATIONAL INACCURACIES (E.G., 200 TIMES THE SLOPE ERROR TOLERANCE OF REFLECTIVE CONCENTRATORS, AND 100 TIMES THE SLOPE ERROR TOLERANCE OF FLAT FRESNEL LENSES), AND EXCELLENT AND SELECTABLE TRACKING ERROR TOLERANCE (1 DEGREE FOR 4 MM CELL, 2 DEGREES FOR 5.4 MM CELL, ETC.)

**CELL USAGE:** VARIOUS CELLS CAN BE USED IN THE DOME LENS CONCENTRATOR, INCLUDING BOEING'S GAAS/GASB, VARIAN'S GAAS, NASA'S INP, ET AL. (DUE TO HIGH CONCENTRATION, ONLY 1% OF NORMAL CELL AREA IS NEEDED).

**PRISMATIC COVERS:** ALLOW HEAVY GRID COVERAGE FOR EFFICIENT CURRENT COLLECTION.

**HEAT REJECTION:** CELLS ARE MOUNTED DIRECTLY TO A BACKSIDE RADIATOR.

**PACKING FACTOR:** LENSES CAN BE CUT SQUARE (OR HEX) IN APERTURE TO MAXIMIZE LENS APERTURE/PANEL AREA RATIO (97% IS EASILY ACHIEVED).

**MODULARITY:** THE NUMBER OF LENS/CELL ELEMENTS CAN BE SELECTED FOR OPTIMAL PANEL OUTPUT.

**MATERIALS:** READILY AVAILABLE LIGHTWEIGHT MATERIALS ARE USED THROUGHOUT THE PANEL.

**MANUFACTURABILITY:** ALL PANEL ELEMENTS APPEAR TO BE READILY MANUFACTURABLE.

**DEPLOYABILITY:** AUTOMATICALLY DEPLOYING STRUCTURES BEING DEVELOPED FOR OTHER CONCENTRATORS CAN BE EASILY ADAPTED TO THE MINI-DOME PANELS. (E.G., THE ASTRO-AEROSPACE ESS OR STACBEAM STRUCTURES).

**COST:** DUE TO THE SMALL CELL AREA REQUIREMENT, THE MASS-PRODUCIBILITY OF ALL ARRAY COMPONENTS, AND THE LARGE ALLOWABLE TOLERANCES, THE MINI-DOME LENS ARRAY OFFERS SIGNIFICANT COST REDUCTION POTENTIAL.

**RADIATION HARDNESS:** THE PANEL CONFIGURATION CAN BE TAILORED TO PROVIDE AN APPROPRIATE LEVEL OF PARTICULATE RADIATION SHIELDING (I.E., ELECTRONS AND PROTONS), MINIMIZING CELL DEGRADATION.